

# Score and Distribution Matching Policy:

## Advanced Accelerated Visuomotor Policies via Matched Distillation

Bofang Jia<sup>1,2,\*</sup> Pengxiang Ding<sup>1,3,\*,\ddagger</sup> Can Cui<sup>1,\*</sup> Mingyang Sun<sup>1,3</sup>

Pengfang Qian<sup>1</sup> Siteng Huang<sup>1</sup> Zhaoxin Fan<sup>4</sup> Donglin Wang<sup>1,\ddagger</sup>

<sup>1</sup>Westlake University <sup>2</sup>Southwest University <sup>3</sup>Zhejiang University

<sup>4</sup>Beijing Advanced Innovation Center for Future Blockchain and Privacy Computing

School of Artificial Intelligence, Beihang University

jiabofang@email.swu.edu.cn, dingpx2015@gmail.com, cuican@westlake.edu.cn

[Project Webpage](#)

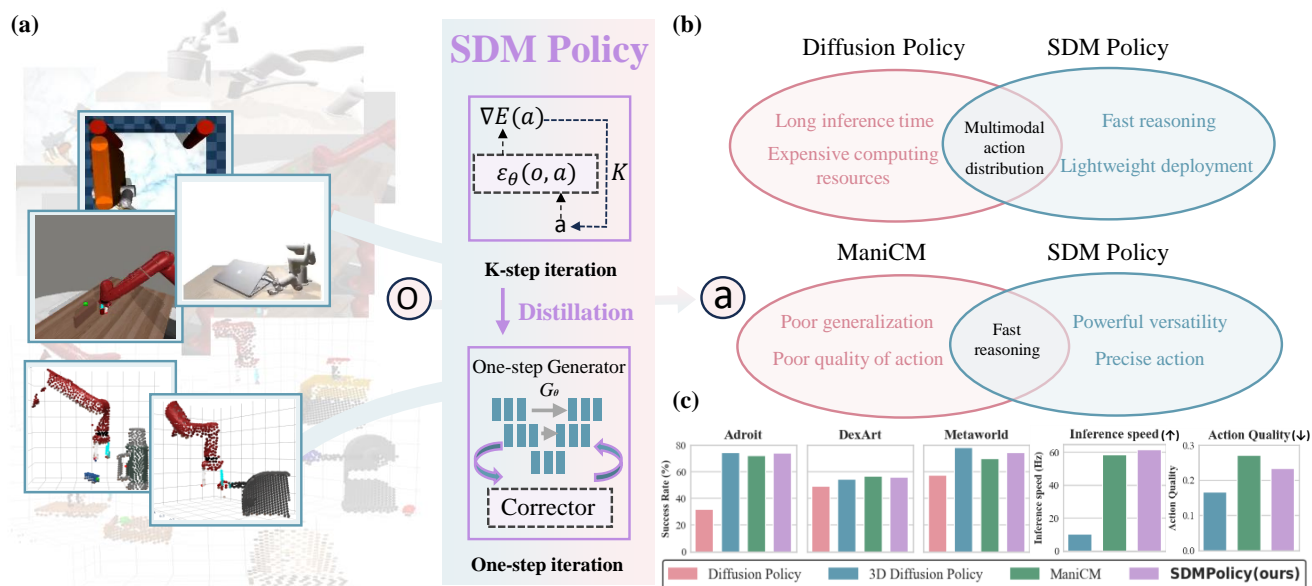


Figure 1. **SDM Policy** is a visual imitation learning algorithm that trains a one-step generator by enforcing a matching loss between two distributions. This approach balances fast inference speed and action accuracy, achieving state-of-the-art performance. (a) illustrates the principle of our method, (b) provides a comparison between SDM Policy, diffusion policy, and current SOTA methods (ManiCM), and (c) demonstrates that our method surpasses the current SOTA in task success rate and inference speed, showing that the quality of our actions is closer to the teacher model, resulting in more accurate action learning.

### Abstract

Visual-motor policy learning has advanced with architectures like diffusion-based policies, known for modeling complex robotic trajectories. However, their prolonged inference times hinder high-frequency control tasks requiring real-time feedback. While consistency distillation (CD) accelerates inference, it introduces errors that compromise

\*Equal contribution.

\ddagger Project Leader.

\ddagger Corresponding author.

action quality. To address these limitations, we propose the Score and Distribution Matching Policy (SDM Policy), which transforms diffusion-based policies into single-step generators through a two-stage optimization process: score matching ensures alignment with true action distributions, and distribution matching minimizes KL divergence for consistency. A dual-teacher mechanism integrates a frozen teacher for stability and an unfrozen teacher for adversarial training, enhancing robustness and alignment with target distributions. Evaluated on a 57-task simulation benchmark, SDM Policy achieves a 6× inference speedup

while having state-of-the-art action quality, providing an efficient and reliable framework for high-frequency robotic tasks. The code and more details can be found at [sdm-policy.github.io](https://github.com/sdm-policy).

## 1. Introduction

Visual-motor policy learning has recently gained significant prominence in robotics, with a range of innovative architectures emerging for exploration, such as diffusion-based [4, 16, 44, 45], flow-matching-based [24], and transformer-based policies [27]. Diffusion-based policies are increasingly recognized for their capability to model intricate, high-dimensional robotic trajectories. This capability allows these policies to capture the complex temporal and spatial dependencies inherent in robotic tasks, providing a robust framework for generating diverse and feasible trajectories under varying task constraints. Therefore, diffusion-based policies have been widely applied to various tasks in robotics, such as grasping [4, 44, 45], and mobile manipulation [22, 40].

However, diffusion-based policies inherently require prolonged inference times, as their step-by-step denoising process involves dozens or even hundreds of forward passes, consuming substantial computational resources and time. This poses a critical limitation for tasks demanding high-frequency control. For instance, tasks such as grasping objects, threading a needle, or picking up moving targets rely on real-time feedback to quickly adjust actions. In scenarios where objects slip or shift position, fast inference is crucial to make immediate corrections.

Currently, many efforts have been made to accelerate diffusion-based policies using consistency distillation (CD) [16, 20], which transfers knowledge from pre-trained teacher models into a single-step sampler. This approach enables rapid one-step generation and significantly improves inference speed. However, CD-based methods are inherently prone to errors due to limitations in their underlying mechanisms. For instance, standard consistency distillation [31] relies on ODE solvers [31], whose numerical approximations can introduce errors, resulting in suboptimal consistency and adversely affecting the model’s overall performance. Similarly, latent consistency distillation [17] is constrained by its focus on local consistency, which restricts the student model’s ability to fully capture and integrate the comprehensive knowledge of the teacher model [10]. These limitations lead to a loss of critical sample information, resulting in a decline in action quality and making it challenging to balance sample quality and inference speed. Consequently, achieving state-of-the-art inference speed while maintaining the accuracy and quality of sample actions is essential.

To solve these problems, we propose **Score and Distri-**

**bution Matching Policy (SDM Policy)**, a framework designed to distill the capabilities of pre-trained diffusion-based teacher models into a single-step generator that is both efficient and accurate. The core of SDM Policy lies in its two-stage optimization process: score matching, which ensures that generated actions closely align with the true action distribution by leveraging the corrected score functions of diffusion policies, and distribution matching, which minimizes the KL divergence between the generator and the teacher policies to enforce distribution-level consistency. Unlike traditional iterative diffusion processes, SDM Policy enables the generator to directly produce high-quality actions in a single step, drastically reducing inference time. Additionally, the method incorporates a frozen teacher model as a stable reference and an unfrozen teacher model to guide the generator’s training through an adversarial optimization framework. This dual-teacher setup ensures the robustness of the generated actions while fostering alignment with the target distribution, thereby enhancing the overall reliability and generalizability of the model. The evaluation of SDM Policy on a 57-task simulation benchmark shows a 6× inference speedup with state-of-the-art action quality.

In summary, our contributions are three-fold:

1. We introduce a framework, SDM Policy, that integrates score and distribution matching to transform diffusion-based policies into efficient single-step generators, enhancing inference speed while retaining action quality.
2. We design a dual-teacher mechanism with a frozen teacher for stability and an unfrozen teacher for adversarial guidance, ensuring robustness and better alignment with the target action distribution.
3. Extensive results show the SDM Policy’s effectiveness on a 57-task benchmark, achieving a 6× inference speedup over standard diffusion policies, with the state-of-the-art action quality.

## 2. Related Work

### 2.1. Diffusion-based Robotic Policy

Currently, visual-based policies [2–5, 10, 11, 13, 16, 23, 24, 28, 32, 37, 46, 47] have successfully tackled challenges in high-dimensional trajectory modeling and complex task decision-making. These advancements have led to the creation of robust and adaptable policy networks, enabling robotic systems to achieve substantial performance improvements across diverse tasks. Diffusion Policy [4] is one of the pioneering works to explore this field, which represents robotic visual-motor policies as a conditional denoising process to generate actions, supporting high-dimensional action spaces and exhibiting impressive training stability. 3D Diffusion Policy [45] extends Diffusion Policy [4] to 3D scenarios by incorporating 3D visual infor-

mation. It efficiently utilizes a compact 3D representation extracted from sparse point clouds with a high-performance point encoder, enhancing performance in robotic imitation learning. Additionally, HDP [18], DNAct [39], and IDP3 [44] extend Diffusion Policy [4] to more complex tasks, showcasing the powerful capability of diffusion policies in handling robotic tasks.

Despite the impressive performance of diffusion models, their costly inference speed has been a barrier for applications in robot tasks that require high real-time capabilities. To address this, a series of works focused on accelerating policies have been developed, and this work also falls into this category.

## 2.2. Accelerated Robotic Policy

Recently, many works have focused on accelerating diffusion policies [8, 16, 20, 36]. The most classic approach to accelerating the policy is to use a consistency model [6, 9, 12, 14, 15, 48], as it can directly map noise to data to generate high-quality samples, enabling fast one-step generation by design. Consistency policy [20], inspired by CTM [10], denoising both back to the same time step  $s$ . Similarly, ManiCM [16] extends the one-step inference into 3D scenarios and achieves faster inference acceleration compared to 3D Diffusion Policy [45]. However, approaches to accelerate using consistency models often result in a loss of sample quality [41], making it challenging to balance speed and generation quality. Therefore, this paper is the first to explore an accelerated policy that maintains action quality while ensuring speed.

## 3. Background

### 3.1. Task Formulation

Robotic manipulation is trained through imitation learning, with a small set of expert demonstrations containing complex skill trajectories utilized to learn a visuomotor policy  $\pi : \mathcal{O} \rightarrow \mathcal{A}$ . This policy maps visual observations  $o \in \mathcal{O}$  to actions  $a \in \mathcal{A}$ , enabling the robot to not only replicate expert skills but also generalize across different environments. The observation includes a combination of point clouds received from an eye-in-hand RGB-D camera and proprioceptive data from the robot or a combination of RGB camera images and proprioceptive data from the robot. The action space varies depending on the task and robot configuration, typically demonstrating SE(3) motion of the end-effector along with the standardized torque to be applied by the gripper fingers.

### 3.2. Diffusion Policy

Diffusion Policy [4] is an advanced vision-based motion policy for robots, designed to generate action sequences in complex tasks. This policy is achieved through a conditional denoising diffusion policy, where given conditions

such as visual features and robot poses, random noise is gradually denoised into the target action sequence. Specifically, starting from a gaussian noise sample, the diffusion model utilizes a noise prediction network  $\pi_\theta$  to predict and remove noise at each step, iterating for  $T$  steps to generate a noise-free action  $a^0$ .

$$a^{t-1} = \alpha_t (a^t - \gamma_t \pi_\theta(a^t, t, v, p)) + \sigma_t \mathcal{N}(0, I), \quad (1)$$

where  $a^t$  denotes the action at step  $T$ ;  $\alpha_t$ ,  $\gamma_t$ , and  $\sigma_t$  are noise scheduling parameters controlling the denoising strength;  $\mathcal{N}(0, I)$  is the noise prediction network used to estimate the noise at each step;  $v$  and  $p$  represent the visual features and robot poses as conditioning information; and  $\mathcal{N}(0, I)$  is gaussian noise.

## 4. Method

In this section, we first provide a detailed explanation of our pipeline and describe the design of each component in our SDM Policy (Section 4.1). To demonstrate the superiority of our approach, we analyze it in comparison with current methods and provide evidence of its effectiveness (Section 4.2).

### 4.1. Score and Distribution Matching Policy

The prolonged inference time of diffusion policies, due to the step-by-step denoising process, hinders their application in dynamic environments requiring high-frequency control and the practical deployment of lightweight robots. Accelerating the diffusion process to enable rapid action generation is essential. Addressing these challenges, our SDM policy achieves fast one-step generation through distribution matching, effectively resolving the slow inference issue of diffusion policies. We will provide a detailed explanation of the SDM policy’s design and training optimization.

#### 4.1.1. Model Architecture

Our SDM policy consists of two main components: the one-step generator and the corrector. The former is responsible for denoising pure noise input in a single step to restore precise actions, while the latter refines the one-step generator during training through gradient and diffusion optimization, ensuring it generates accurate actions comparable to those of the teacher model. The overall pipeline of SDM Policy is illustrated in Figure 2, effectively addressing the low decision-making efficiency in diffusion policies.

**One-step generator.** Our method distills the diffusion policies, which require long inference times and high computational costs, into a fast and stable one-step generator. The one-step generator starts from pure noise  $z$  and generates accurate actions  $a_\theta^0$  through single-step denoising, implemented by the generator  $G_\theta$ . To further improve the accuracy of action generation, we introduce a Corrector mechanism during training, which provides fine adjustments to



Figure 2. **Overview of SDM Policy.** Our method distills diffusion policies, which require long inference times and high computational costs, into a fast and stable one-step generator. Our SDM Policy is represented by the one-step generator, which requires continual correction and optimization via the Corrector during training, but relies solely on the generator during evaluation. The corrector’s optimization is based on two components: gradient optimization and diffusion optimization. The gradient optimization part primarily involves optimizing the entire distribution by minimizing the KL divergence between two distributions,  $P_\theta$  and  $D_\theta$ , with distribution details represented through a score function that guides the gradient update direction, providing a clear signal. The diffusion optimization component enables  $D_\theta$  to quickly track changes in the one-step generator’s output, maintaining consistency. Details on loading observational data for both evaluation and training processes are provided above the diagram. Our method applies to both 2D and 3D scenarios.

the outputs of the one-step generator, ensuring the precision of the generated actions.

**Corrector.** To achieve more accurate action generation within the one-step generation framework, we introduce a unique Corrector structure. This Corrector consists of two networks,  $P_\theta$  and  $D_\theta$ , which work together like adversarial generation. By comparing the outputs of these two networks, the Corrector determines the necessary action adjustments, serving as explicit labels for refinement. Both  $P_\theta$  and  $D_\theta$  are constructed based on the pre-trained diffusion policies  $\pi_\theta$ , with  $P_\theta$  remaining fixed while  $D_\theta$  continuously updates its parameters to adapt to the generator’s outputs.

To guide the learning process, we leverage the known properties of the diffusion model to approximate the score function over the diffusion distribution. This allows us to interpret the denoised output as the gradient direction, thereby guiding the Corrector’s adjustments. We use the KL divergence to measure the difference between the distributions represented by  $P_\theta$  and  $D_\theta$ , providing detailed updates for the generator’s output action  $a_{G(\theta)}^0$ . This ensures that actions are generated in a more realistic direction. Finally, the gradient updates for our one-step generator are set to

this difference, obtaining the necessary details for updating the generated actions and ensuring that the labels directly impact the training process of our one-step generator, gradually reducing the loss of learning information.

$$\begin{aligned}
 D_{\text{KL}}(p_{D_\theta} \| p_{P_\theta}) &= \mathbb{E} \left( \log \left( \frac{p_{D_\theta}(a_{G(\theta)}^t)}{p_{P_\theta}(a_{G(\theta)}^t)} \right) \right) \\
 &= \mathbb{E}_{z \sim \mathcal{N}(0, \mathbf{I})} \left[ - \left( \log p_{P_\theta}(a_{G(\theta)}^t) - \log p_{D_\theta}(a_{G(\theta)}^t) \right) \right]. \quad (2)
 \end{aligned}$$

#### 4.1.2. Training Strategy

In the training phase, we progressively optimize the one-step generator through two components, enabling it to achieve impressive action generation.

**Gradient optimization.** We face two challenges in gradient computation. First, real-world data often lies on a low-dimensional manifold within a high-dimensional ambient space [29]. The score  $\nabla_x \log p_{\text{data}}(x)$  represents the gradient in this ambient space, so it becomes undefined when  $x$  is limited to the low-dimensional manifold. Consequently, data sparsity in low-density regions results in inaccurate score matching (Figure 3). Additionally, since our distributions use diffusion policy as a base model, the scores corre-

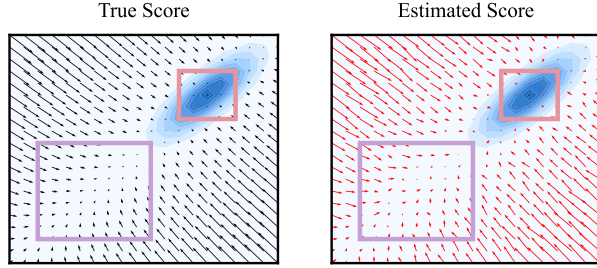


Figure 3. **Performance of score estimation in low-density regions.** The purple rectangle represents low-density regions, and the pink rectangle represents high-density regions. For the entire rectangle, darker colors indicate higher density. The left image shows the true data scores, while the right image shows the estimated scores. In the high-density pink rectangle, the difference between the estimated and true scores is minimal. However, in the low-density purple rectangle, the difference between the estimated and true scores is significantly larger, indicating poor score matching performance in low-density regions.

respond to diffused distributions rather than the original, complicating accurate gradient estimation. To address these issues, we perturb the data with gaussian noise at varying levels, enabling score calculation in overlapping regions where both distributions’ scores can be simultaneously computed [29, 42].

Score computation refers to the process where, in the reverse denoising process, the model estimates the score  $s(a^t)$  to determine the denoising direction at each step, ultimately recovering the original noiseless sample. The score estimate  $s(a^t)$  provides a way to return from the noisy data  $a^t$  to the noise-free action  $a^0$ . In practical applications [30], the score estimate can be expressed by the following formula:

$$s(a^t) = \frac{a^t - \alpha_t \pi_\theta(a^t, t, v, p)}{\sigma_t^2}, \quad (3)$$

where  $\pi_\theta$  represents the trained diffusion policies,  $\alpha_t$  and  $\sigma_t$  are noise scheduling parameters controlling the denoising strength,  $v$  and  $p$  represent the visual features and robot poses as conditioning information. Now, we only need the gradient with respect to  $\theta$  to train our one-step generator through gradient descent.

$$\begin{aligned} \nabla_\theta D_{\text{KL}} &= \mathbb{E}_{z \sim \mathcal{N}(0, \mathbf{I})} [-(s_{P_\theta}(a_{G(\theta)}^t) - s_{D_\theta}(a_{G(\theta)}^t)) \nabla_\theta G_\theta(z)] \\ &= \mathbb{E}_{z \sim \mathcal{N}(0, \mathbf{I})} [-(a_{P(\theta)}^0 - a_{D(\theta)}^0) \nabla_\theta G_\theta(z)] \end{aligned} \quad (4)$$

$$\mathcal{L}_{\text{one-step generator}} = \lambda \nabla_\theta D_{\text{KL}}, \quad (5)$$

where  $\lambda$  is a scaling factor for the one-step generator loss. **Diffusion loss optimization.** For the dynamically changing  $D_\theta$  in the corrector, the distribution of the generated actions changes throughout the training process. We need to continuously update  $D_\theta$  to adapt to these changes, ensuring that the output  $a_{D(\theta)}^0$  of  $D_\theta$  remains consistent with the output

$a_{G(\theta)}^0$  of the one-step generator. During training, we update the parameters  $\theta$  by minimizing the standard denoising objective [7, 34]:

$$\mathcal{L}_{\text{Diffusion}} = \gamma \text{MSE}(a_{D(\theta)}^0, a_{G(\theta)}^0), \quad (6)$$

where  $\gamma$  is a scaling factor for the diffusion loss.

## 4.2. Foundations and Comparative Analysis

To better demonstrate the effectiveness of our method, we will conduct a discussion from two perspectives: theoretical analysis and comparative analysis with current state-of-the-art methods.

**Theoretical foundations.** To accelerate inference more effectively, numerous approaches have been attempted in the field of robotics for diffusion policies, including methods such as consistency distillation and latent consistency distillation for one-step generation. However, distillation for generative tasks often yields suboptimal results, failing to achieve the accurate action generation and multimodal action capabilities of the original diffusion policies. We found that this is because model optimization relies solely on distillation loss, lacking a direct signal similar to data labels in classification tasks. In this situation, the student model struggles to capture the details and diversity necessary for generating samples, resulting in decreased action accuracy and multimodal capability.

To address this shortcoming, our method offers an effective solution by leveraging classification to provide the one-step generator with direct supervision signals. Beyond simple distillation loss, we introduce a signal similar to classification loss to guide the policy toward realistic action generation, enabling continual optimization for greater accuracy. In our corrector structure, we use KL divergence to align the generated action distribution with the target distribution. This approach allows the one-step generator to learn an action policy consistent with the true distribution, even with limited expert demonstration data, thereby enhancing the diversity and generalization of generated behaviors.

**Limitations of existing methods.** The current state-of-the-art methods for accelerating diffusion policies are consistency distillation and latent consistency distillation, but both suffer from inevitable temporal errors, making it challenging to achieve accurate action generation and multimodal action generation capabilities through distillation in diffusion policies (Figure 4).

A major limitation of consistency distillation lies in the unavoidable accumulation of errors due to its reliance on a discrete consistency model. This discrete-time model is sensitive to the choice of  $\Delta t$ . The noise sample at the previous time step  $t - \Delta t$ , denoted as  $a_{t-\Delta t}$ , is derived from  $a_t$  by solving the PF-ODE with a numerical ODE solver and a step size of  $\Delta t$ . This approach introduces discretization errors, resulting in inaccurate predictions during training.

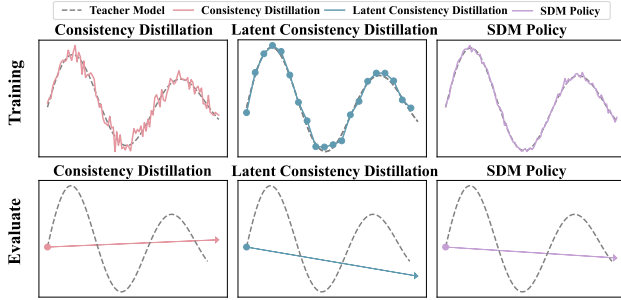


Figure 4. **Comparison of SDM Policy and consistent distillation.** Here we provide a detailed comparison of the differences in the training process between consistency distillation, latent consistency distillation, and our SDM Policy. Consistency distillation suffers from significant deviations in one-step generation due to error accumulation, while latent consistency distillation quickly overlooks the need for global consistency. In contrast, our method aligns and learns at the distribution level, effectively addressing the issues mentioned above.

Since all solvers inherently introduce such errors, improving the solver is challenging, limiting the ability to achieve high-quality results in a few steps and hindering effective application.

In contrast, latent consistency distillation is constrained by local consistency, aligning only at intervals of  $k$  steps. This introduces skip-step errors and aligns with the pre-trained model locally, lacking a global structural perspective. As a result, the quality and diversity of generated samples are compromised. Our method avoids these issues by eliminating stepwise error accumulation and local consistency limitations. Instead, we employ global consistency by learning the entire distribution of the diffusion policies and optimizing solely at the distribution level through KL divergence, achieving more efficient and robust improvement.

## 5. Experiments

In this section, we first introduce the experimental setup, including the dataset, baseline methods, evaluation metrics, and implementation details (Section 5.1). Then, we demonstrate the efficiency and effectiveness of our method in detail through experiments, along with visualized results from the experimental process (Section 5.2). Finally, we conduct an ablation study to explore the impact of different design choices within our method (Section 5.3). In the main text, we provide a detailed description of the 57 tasks associated with 3D Diffusion Policy [45]. For the 2D policy, we include it solely to demonstrate the generalizability of our method, indicating that it can distill any diffusion policies. Detailed results can be found in the supplementary material A.

### 5.1. Experimental Setup

To comprehensively and objectively evaluate our model, we set up 57 robotic tasks across three domains. This is primarily to ensure that our model is tested on a more scientifically rigorous benchmark, despite the fact that today’s simulated tasks are increasingly realistic [33, 38, 45, 49].

**Datasets.** The 57 robotic tasks across three domains are sourced from Adroit [21], DexArt [1], and MetaWorld [43]. Specifically, we use reinforcement learning VRL3 [35], to obtain expert demonstrations for Adroit, while for MetaWorld tasks, we present results from scripted policies. According to [26], MetaWorld tasks are categorized into different difficulty levels ranging from simple to very challenging. DexArt uses PPO [25] for trajectory generation. For each benchmark, we use a limited set of 10 expert demonstrations for training.

**Baselines.** To balance fast inference speed with accurate actions and to validate the effectiveness of our method, our benchmarks primarily include the advanced point cloud-based Diffusion Policy (DP3) [45], and one-step generation model ManiCM [16], generated through consistency distillation.

**Evaluation metrics.** For each random seed, we evaluate 20 segments every 200 training epochs, then calculate the average success rate of the top 5 segments as well as the average runtime for each task\*. To ensure the fairness of the experiments, we randomly run three seeds for each task experiment, consistent with previous work [16, 45].

### 5.2. Efficiency and Effectiveness

To demonstrate the effectiveness of our method, we conducted a comprehensive evaluation across four key aspects: task success rate, learning efficiency, inference time, and action learning. SDM Policy exhibited strong performance across all these areas. In the table, results highlighted in bold indicate the top-performing method, while results with an underline denote the second best performance across the various categories.

**High accuracy.** Table 1 presents the overall results for the 57 tasks across 3 domains. Compared to diffusion-based policies represented by DP3 and consistency-based policies represented by ManiCM, our method achieved a higher success rate across multiple tasks. Additionally, we randomly selected 20 tasks proportional to the number of tasks in each domain; the detailed results are shown in Table 2. A complete report of the success rates for each task can be found in the supplementary material.

**Learning efficiency.** Figure 5 shows the results after 3000 epochs of training. We observed that the SDM Policy achieved a faster convergence rate compared to others. Fur-

\*All of our task training and evaluation were conducted on an NVIDIA A100 80G GPU.

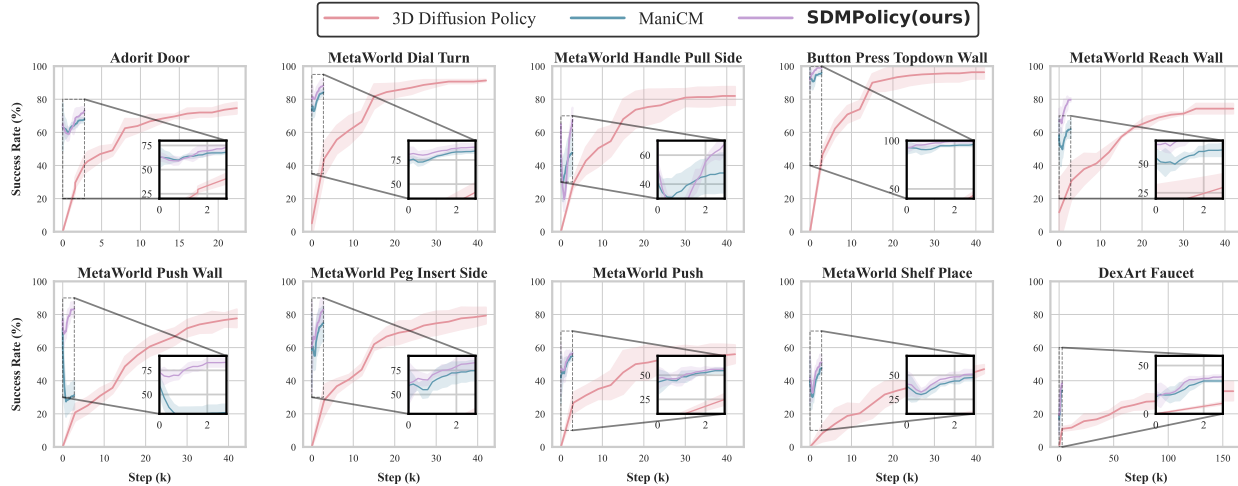


Figure 5. **Learning efficiency.** We sampled 10 simulation tasks and presented the learning curves of our SDM Policy alongside DP3 and ManiCM. SDM Policy demonstrated a rapid convergence rate. In contrast, ManiCM showed slower learning progress, and DP3’s convergence speed was also slower than our method.

Table 1. **Comparisons on success rate.** We evaluated 57 challenging tasks using 3 random seeds and reported the average success rate (%) and standard deviation for three domains. \* indicates our reproduction of that task. Our SDM Policy outperforms the current state-of-the-art model in one-step inference, achieving better results than Consistency Distillation and coming closer to the performance of the teacher model, which demonstrates its effectiveness.

Method	NFE	Adroit (3)	DexArt (4)	Metaworld Easy (28)	Metaworld Medium (11)	Metaworld Hard (6)	Metaworld Very Hard (5)	Average
Diffusion Policy [4]	10	31.7	49.0	83.6	31.1	9.0	26.6	$55.5 \pm 3.58$
3D Diffusion Policy [45]	10	68.3	68.5	90.9	61.6	31.7	49.0	$72.6 \pm 3.20$
3D Diffusion Policy*	10	<b>74.3</b>	54.3	<b>89.0</b>	<b>72.7</b>	<b>38.0</b>	<b>75.8</b>	<b><math>76.1 \pm 2.32</math></b>
ManiCM*	1	72.3	<b>56.8</b>	83.6	55.6	33.3	67.0	$69.0 \pm 4.60$
<b>SDM Policy</b>	1	<u>74.0</u>	<u>56.0</u>	<u>86.5</u>	<u>65.8</u>	<u>35.8</u>	<u>71.6</u>	<u><math>74.8 \pm 4.51</math></u>

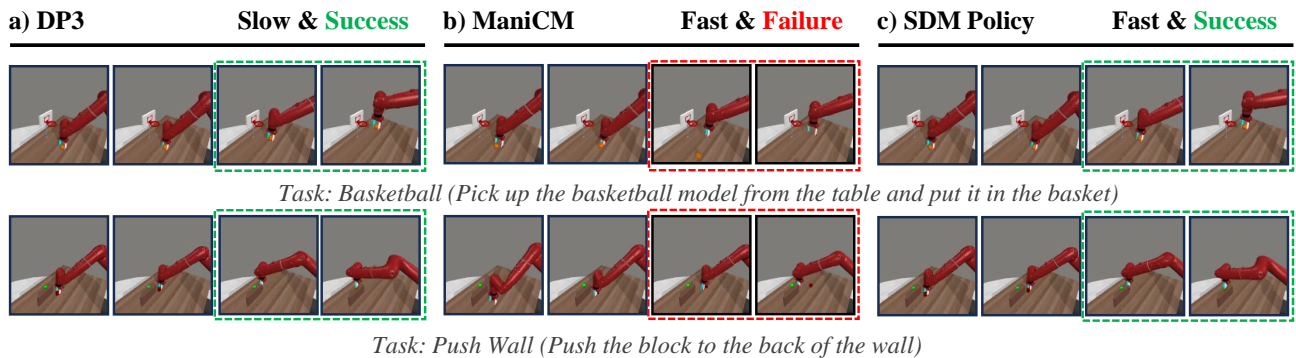


Figure 6. **Task execution visualization.** Visualized keyframes for Basketball and Push Wall tasks, we found that during training, our SDM Policy could better complete the task and learn more precise actions, while consistency distillation might lead to task failure.

thermore, our SDM Policy distillation performance is closer to that of the teacher model than ManiCM.

**Competitive inference speed.** Table 3 presents the overall inference speed results for the 57 tasks. Compared to diffusion-based policies represented by DP3 and consistency-based policies represented by ManiCM, our method achieves inference speeds on par with the state-

of-the-art ManiCM, enabling rapid inference while being approximately 6 times faster than the diffusion-based DP3. Detailed inference times for individual tasks can be found in the supplementary material.

**Precise and accurate action.** As shown in Table 4, we also found that the action quality learned by SDM Policy is approximately better than that of ManiCM, the

Table 2. **Success rate results for detailed experiments.** We provided a detailed presentation of the success rate (%) and standard deviation for some tasks, with \* indicating our reproduction of that task. The tasks were selected from different parts of the 57 tasks, and we randomly chose 20 tasks according to the corresponding proportion for demonstration. The results demonstrate the broad effectiveness of our approach on both simple grasping and pushing-pulling operations, as well as complex dexterous hand tasks.

Algorithm \ Task	Adroit		MetaWorld (Easy)							
	Door	Pen	Dial-Turn	Door-Unlock	Handle-Pull	Handle-Pull-Side	Lever-Pull	Reach-Wall	Window-Open	Peg-Unplug-Side
3D Tasks										
Diffusion Policy [4]	37 ± 2	13 ± 2	63 ± 10	98 ± 3	27 ± 22	23 ± 17	49 ± 5	59 ± 7	100 ± 0	74 ± 3
3D Diffusion Policy [45]	62 ± 4	43 ± 6	66 ± 1	100 ± 0	53 ± 11	85 ± 3	79 ± 8	68 ± 3	100 ± 0	75 ± 5
3D Diffusion Policy*	<b>75 ± 3</b>	<b>48 ± 3</b>	<b>91 ± 0</b>	<b>100 ± 0</b>	<b>52 ± 8</b>	<b>82 ± 5</b>	<b>84 ± 8</b>	<b>74 ± 3</b>	<b>99 ± 1</b>	<b>93 ± 3</b>
ManiCM*	68 ± 1	49 ± 4	84 ± 2	82 ± 16	10 ± 10	48 ± 11	82 ± 7	62 ± 5	80 ± 26	71 ± 15
<b>SDM Policy (Ours)</b>	<b>73 ± 2</b>	<b>42 ± 3</b>	<b>88 ± 3</b>	<b>95 ± 6</b>	<b>28 ± 11</b>	<b>68 ± 6</b>	<b>84 ± 9</b>	<b>80 ± 1</b>	78 ± 18	<b>74 ± 19</b>

Algorithm \ Task	MetaWorld (Medium)				MetaWorld (Hard)		MetaWorld (Very Hard)		DexArt		Average
	Peg-Insert-Side	Coffee-Pull	Push-Wall	Sweep	Pick-Out-Of-Hole	Push	Shelf-Place	Stick-Pull	Faucet	Bucket	
3D Tasks											
Diffusion Policy [4]	30 ± 5	34 ± 7	20 ± 3	18 ± 8	0 ± 0	30 ± 3	11 ± 3	11 ± 2	23 ± 8	46 ± 1	38.4
3D Diffusion Policy [45]	42 ± 3	87 ± 3	49 ± 8	96 ± 3	14 ± 9	51 ± 3	17 ± 10	27 ± 8	63 ± 2	46 ± 2	71.2
3D Diffusion Policy*	<b>79 ± 4</b>	<b>79 ± 2</b>	<b>78 ± 5</b>	<b>92 ± 4</b>	<b>44 ± 3</b>	<b>56 ± 5</b>	47 ± 2	<b>67 ± 0</b>	34 ± 5	29 ± 2	<b>70.1</b>
ManiCM*	75 ± 8	68 ± 18	31 ± 7	54 ± 16	30 ± 6	55 ± 2	48 ± 3	63 ± 2	34 ± 0	36 ± 4	56.7
<b>SDM Policy (Ours)</b>	<b>83 ± 5</b>	<b>72 ± 9</b>	<b>83 ± 4</b>	<b>90 ± 6</b>	<b>34 ± 24</b>	<b>57 ± 0</b>	<b>51 ± 4</b>	<b>68 ± 10</b>	<b>38 ± 1</b>	<b>31 ± 3</b>	<b>65.9</b>

Table 3. **Comparisons on inference speed.** We evaluated 57 challenging tasks using 3 random seeds and reported the average speed (Hz) for three domains. \* indicates our reproduction of that task, and - indicates that the data for this method has not been disclosed. Our SDM Policy outperforms the current state-of-the-art model in one-step inference, achieving better results than Consistency Distillation, providing strong evidence of the effectiveness of our model.

Method	NFE	Adroit (3)	DexArt (4)	Metaworld Easy (28)	Metaworld Medium (11)	Metaworld Hard (6)	Metaworld Very Hard (5)	Average
Diffusion Policy [4]	10	-	-	-	-	-	-	-
3D Diffusion Policy [45]	10	-	-	-	-	-	-	-
3D Diffusion Policy*	10	10.79Hz	10.62Hz	10.01Hz	10.79Hz	10.92Hz	10.53Hz	10.39Hz
ManiCM*	1	<b>57.56Hz</b>	<b>73.19Hz</b>	<b>55.03Hz</b>	<b>60.32Hz</b>	<b>66.26Hz</b>	<b>57.16Hz</b>	<b>58.48Hz</b>
<b>SDM Policy</b>	1	<b>57.47Hz</b>	<b>75.59Hz</b>	<b>62.20Hz</b>	<b>60.06Hz</b>	<b>65.91Hz</b>	<b>52.06Hz</b>	<b>61.75Hz</b>

Table 4. **Comparisons on action.** We used 3 random seeds to compare the learning effects of action generation on a 57 challenging task during training, and reported the mean action error and standard deviation in the three domains. \* indicates our reproduction of that task. Our SDM Policy outperforms current state-of-the-art models in one-step inference and achieves better results than Consistency Distillation.

Method	NFE	Adroit (3)	DexArt (4)	Metaworld (50)	Average
3D Diffusion Policy*	10	<b>0.055 ± 0.037</b>	0.017 ± 0.005	<b>0.182 ± 0.311</b>	<b>0.166 ± 0.278</b>
ManiCM*	1	<b>0.179 ± 0.001</b>	<b>0.010 ± 0.000</b>	0.298 ± 0.016	0.270 ± 0.014
<b>SDM Policy</b>	1	0.179 ± 0.008	<b>0.010 ± 0.000</b>	<b>0.251 ± 0.019</b>	<b>0.234 ± 0.017</b>

Table 5. **Ablation on generator config.** We conduct training from scratch on the one-step generator to evaluate the impact of the pre-trained policy, reporting the overall task success rate, inference speed, and action quality.

Method	success rate	inference speed	action
SDM Policy	63.7 ± 2.7	65.44Hz	0.100 ± 0.007
w/o generator config	58.0 ± 4.0	51.19Hz	0.227 ± 0.013

consistency-distilled model. This improvement indicates that our method preserves much more information during distillation, aligning with the previously noted higher success rates and learning efficiency, further validating the effectiveness of our approach. Detailed reports on action learning performance for individual tasks can be found in

the supplementary material.

For task execution performance, we provide a detailed illustration in Figure 6. For certain tasks, our SDM Policy better captures the action execution of the teacher model, while the consistency distillation method may encounter task execution failures.

### 5.3. Ablation Studies

In SDM Policy, we specifically load the parameters of the pre-trained policy  $\pi_\theta$  to initialize our one-step generator  $G_\theta$ . To compare initialization methods for the one-step generator, validate, and explore our design choices, we selected seven tasks for experimentation: Adroit Door from Adroit, and Box-Close, Push, Reach, Reach Wall, Shelf-Place, and Sweep from MetaWorld. As shown in Table 5, methods that do not load the parameters of the pre-trained policy  $\pi_\theta$  fail to meet our requirements for rapid generation and high-quality actions, indicating the critical importance of properly utilizing pre-trained policy parameters.

## 6. Discussion and Conclusion

This work has demonstrated that enforcing the minimization of the matching loss between two diffusion distributions to provide direct signals for training the generator can significantly improve distillation performance. By addressing various robotic tasks in simulated



environments, it has been shown that our method achieves a balance between fast inference speed and high-quality, precise actions, delivering SOTA results across all metrics. However, some unresolved issues remain worth exploring. All tasks in our simulation benchmark involve static objects and pre-defined environments, which limit the scope of validation to controlled settings. For practical applications, it is crucial to extend the approach to dynamic operations and tasks requiring high-frequency control to adapt to more complex and unpredictable environments. This may involve adopting different update frequencies to address challenges in our gradient optimization and diffusion optimization, which will serve as a primary direction for future work.

## References

- [1] Chen Bao, Helin Xu, Yuzhe Qin, and Xiaolong Wang. Dextar: Benchmarking generalizable dexterous manipulation with articulated objects, 2023. [6](#), [1](#)
- [2] Anthony Brohan, Noah Brown, Justice Carbajal, Yevgen Chebotar, Xi Chen, Krzysztof Choromanski, Tianli Ding, Danny Driess, Avinava Dubey, Chelsea Finn, Pete Florence, Chuyuan Fu, Montse Gonzalez Arenas, Keerthana Gopalakrishnan, Kehang Han, Karol Hausman, Alexander Herzog, Jasmine Hsu, Brian Ichter, Alex Irpan, Nikhil Joshi, Ryan Julian, Dmitry Kalashnikov, Yuheng Kuang, Isabel Leal, Lisa Lee, Tsang-Wei Edward Lee, Sergey Levine, Yao Lu, Henryk Michalewski, Igor Mordatch, Karl Pertsch, Kanishka Rao, Krista Reymann, Michael Ryoo, Grecia Salazar, Pannag Sanketi, Pierre Sermanet, Jaspier Singh, Anikait Singh, Radu Soricut, Huong Tran, Vincent Vanhoucke, Quan Vuong, Ayzaan Wahid, Stefan Welker, Paul Wohlhart, Jialin Wu, Fei Xia, Ted Xiao, Peng Xu, Sichun Xu, Tianhe Yu, and Brianna Zitkovich. Rt-2: Vision-language-action models transfer web knowledge to robotic control, 2023. [2](#)
- [3] Anthony Brohan, Noah Brown, Justice Carbajal, Yevgen Chebotar, Joseph Dabis, Chelsea Finn, Keerthana Gopalakrishnan, Karol Hausman, Alex Herzog, Jasmine Hsu, Julian Ibarz, Brian Ichter, Alex Irpan, Tomas Jackson, Sally Jesmonth, Nikhil J Joshi, Ryan Julian, Dmitry Kalashnikov, Yuheng Kuang, Isabel Leal, Kuang-Huei Lee, Sergey Levine, Yao Lu, Utsav Malla, Deeksha Manjunath, Igor Mordatch, Ofir Nachum, Carolina Parada, Jodilyn Peralta, Emily Perez, Karl Pertsch, Jornell Quiambao, Kanishka Rao, Michael Ryoo, Grecia Salazar, Pannag Sanketi, Kevin Sayed, Jaspier Singh, Sumedh Sontakke, Austin Stone, Clayton Tan, Huong Tran, Vincent Vanhoucke, Steve Vega, Quan Vuong, Fei Xia, Ted Xiao, Peng Xu, Sichun Xu, Tianhe Yu, and Brianna Zitkovich. Rt-1: Robotics transformer for real-world control at scale, 2023.
- [4] Cheng Chi, Siyuan Feng, Yilun Du, Zhenjia Xu, Eric Cousineau, Benjamin Burchfiel, and Shuran Song. Diffusion policy: Visuomotor policy learning via action diffusion. In *Proceedings of Robotics: Science and Systems (RSS)*, 2023. [2](#), [3](#), [7](#), [8](#), [1](#)
- [5] Pengxiang Ding, Han Zhao, Wenxuan Song, Wenjie Zhang, Min Zhang, Siteng Huang, Ningxi Yang, and Donglin Wang. Quar-vla: Vision-language-action model for quadruped robots, 2024. [2](#)
- [6] Zhongjie Duan, Chengyu Wang, Cen Chen, Jun Huang, and Weining Qian. Optimal linear subspace search: Learning to construct fast and high-quality schedulers for diffusion models. In *Proceedings of the 32nd ACM International Conference on Information and Knowledge Management*, page 463–472. ACM, 2023. [3](#)
- [7] Jonathan Ho, Ajay Jain, and Pieter Abbeel. Denoising diffusion probabilistic models. *NeurIPS*, 2020. [5](#)
- [8] Sigmund H. Høeg, Yilun Du, and Olav Egeland. Streaming diffusion policy: Fast policy synthesis with variable noise diffusion models, 2024. [3](#)
- [9] Tero Karras, Miika Aittala, Timo Aila, and Samuli Laine. Elucidating the design space of diffusion-based generative models, 2022. [3](#)
- [10] Dongjun Kim, Chieh-Hsin Lai, Wei-Hsiang Liao, Naoki Murata, Yuhta Takida, Toshimitsu Uesaka, Yutong He, Yuki Mitsufuji, and Stefano Ermon. Consistency trajectory models: Learning probability flow ode trajectory of diffusion. *arXiv preprint arXiv:2310.02279*, 2023. [2](#), [3](#)
- [11] Moo Jin Kim, Karl Pertsch, Siddharth Karamcheti, Ted Xiao, Ashwin Balakrishna, Suraj Nair, Rafael Rafailov, Ethan Foster, Grace Lam, Pannag Sanketi, Quan Vuong, Thomas Kollar, Benjamin Burchfiel, Russ Tedrake, Dorsa Sadigh, Sergey Levine, Percy Liang, and Chelsea Finn. Openvla: An open-source vision-language-action model, 2024. [2](#)
- [12] Luping Liu, Yi Ren, Zhijie Lin, and Zhou Zhao. Pseudo numerical methods for diffusion models on manifolds, 2022. [3](#)
- [13] Songming Liu, Lingxuan Wu, Bangguo Li, Hengkai Tan, Huayu Chen, Zhengyi Wang, Ke Xu, Hang Su, and Jun Zhu. Rdt-1b: a diffusion foundation model for bimanual manipulation, 2024. [2](#)
- [14] Cheng Lu, Yuhao Zhou, Fan Bao, Jianfei Chen, Chongxuan Li, and Jun Zhu. Dpm-solver: A fast ode solver for diffusion probabilistic model sampling in around 10 steps, 2022. [3](#)
- [15] Cheng Lu, Yuhao Zhou, Fan Bao, Jianfei Chen, Chongxuan Li, and Jun Zhu. Dpm-solver++: Fast solver for guided sampling of diffusion probabilistic models, 2023. [3](#)
- [16] Guanxing Lu, Zifeng Gao, Tianxing Chen, Wenxun Dai, Ziwei Wang, and Yansong Tang. Manicm: Real-time 3d diffusion policy via consistency model for robotic manipulation. *arXiv preprint arXiv:2406.01586*, 2024. [2](#), [3](#), [6](#)
- [17] Simian Luo, Yiqin Tan, Longbo Huang, Jian Li, and Hang Zhao. Latent consistency models: Synthesizing high-resolution images with few-step inference, 2023. [2](#)
- [18] Xiao Ma, Sumit Patidar, Iain Haughton, and Stephen James. Hierarchical diffusion policy for kinematics-aware multi-task robotic manipulation. *CVPR*, 2024. [3](#)
- [19] Ajay Mandlekar, Danfei Xu, Josiah Wong, Soroush Nasiriany, Chen Wang, Rohun Kulkarni, Li Fei-Fei, Silvio Savarese, Yuke Zhu, and Roberto Martín-Martín. What matters in learning from offline human demonstrations for robot manipulation. In *arXiv preprint arXiv:2108.03298*, 2021. [3](#)
- [20] Aaditya Prasad, Kevin Lin, Jimmy Wu, Linqi Zhou, and Jeannette Bohg. Consistency policy: Accelerated visuomotor

- tor policies via consistency distillation. In *Robotics: Science and Systems*, 2024. 2, 3
- [21] Aravind Rajeswaran, Vikash Kumar, Abhishek Gupta, Giulia Vezzani, John Schulman, Emanuel Todorov, and Sergey Levine. Learning complex dexterous manipulation with deep reinforcement learning and demonstrations. *arXiv preprint arXiv:1709.10087*, 2017. 6, 1
- [22] Yajvan Ravan, Zhutian Yang, Tao Chen, Tomás Lozano-Pérez, and Leslie Pack Kaelbling. Combining planning and diffusion for mobility with unknown dynamics, 2024. 2
- [23] Allen Z. Ren, Justin Lidard, Lars L. Ankile, Anthony Simeonov, Pulkit Agrawal, Anirudha Majumdar, Benjamin Burchfiel, Hongkai Dai, and Max Simchowitz. Diffusion policy optimization, 2024. 2
- [24] Quentin Rouxel, Andrea Ferrari, Serena Ivaldi, and Jean-Baptiste Mouret. Flow matching imitation learning for multi-support manipulation, 2024. 2
- [25] John Schulman, Filip Wolski, Prafulla Dhariwal, Alec Radford, and Oleg Klimov. Proximal policy optimization algorithms, 2017. 6
- [26] Younggyo Seo, Danijar Hafner, Hao Liu, Fangchen Liu, Stephen James, Kimin Lee, and Pieter Abbeel. Masked world models for visual control, 2023. 6
- [27] Nur Muhammad Mahi Shafiullah, Zichen Jeff Cui, Ariuntuya Altanzaya, and Lerrel Pinto. Behavior transformers: Cloning  $k$  modes with one stone, 2022. 2
- [28] Wenxuan Song, Han Zhao, Pengxiang Ding, Can Cui, Shangke Lyu, Yaning Fan, and Donglin Wang. Germ: A generalist robotic model with mixture-of-experts for quadruped robot, 2024. 2
- [29] Yang Song and Stefano Ermon. Generative modeling by estimating gradients of the data distribution, 2020. 4, 5
- [30] Yang Song, Jascha Sohl-Dickstein, Diederik P Kingma, Abhishek Kumar, Stefano Ermon, and Ben Poole. Score-based generative modeling through stochastic differential equations. In *International Conference on Learning Representations*, 2021. 5
- [31] Yang Song, Prafulla Dhariwal, Mark Chen, and Ilya Sutskever. Consistency models, 2023. 2
- [32] Octo Model Team, Dibya Ghosh, Homer Walke, Karl Pertsch, Kevin Black, Oier Mees, Sudeep Dasari, Joey Hejna, Tobias Kreiman, Charles Xu, Jianlan Luo, You Liang Tan, Lawrence Yunliang Chen, Pannag Sanketi, Quan Vuong, Ted Xiao, Dorsa Sadigh, Chelsea Finn, and Sergey Levine. Octo: An open-source generalist robot policy, 2024. 2
- [33] Emanuel Todorov, Tom Erez, and Yuval Tassa. Mujoco: A physics engine for model-based control. In *2012 IEEE/RSJ International Conference on Intelligent Robots and Systems*, pages 5026–5033, 2012. 6
- [34] Pascal Vincent. A connection between score matching and denoising autoencoders. *Neural Computation*, 23(7):1661–1674, 2011. 5
- [35] Che Wang, Xufang Luo, Keith Ross, and Dongsheng Li. Vrl3: A data-driven framework for visual deep reinforcement learning, 2023. 6
- [36] Zhendong Wang, Zhaoshuo Li, Ajay Mandlekar, Zhenjia Xu, Jiaojiao Fan, Yashraj Narang, Linxi Fan, Yuke Zhu, Yogesh Balaji, Mingyuan Zhou, Ming-Yu Liu, and Yu Zeng. One-step diffusion policy: Fast visuomotor policies via diffusion distillation, 2024. 3
- [37] Junjie Wen, Yichen Zhu, Jinming Li, Minjie Zhu, Kun Wu, Zhiyuan Xu, Ning Liu, Ran Cheng, Chaomin Shen, Yaxin Peng, Feifei Feng, and Jian Tang. Tinyvla: Towards fast, data-efficient vision-language-action models for robotic manipulation, 2024. 2
- [38] Fanbo Xiang, Yuzhe Qin, Kaichun Mo, Yikuan Xia, Hao Zhu, Fangchen Liu, Minghua Liu, Hanxiao Jiang, Yifu Yuan, He Wang, Li Yi, Angel X. Chang, Leonidas J. Guibas, and Hao Su. Sapien: A simulated part-based interactive environment, 2020. 6
- [39] Ge Yan, Yueh-Hua Wu, and Xiaolong Wang. Dnact: Diffusion guided multi-task 3d policy learning, 2024. 3
- [40] Jingyun Yang, Zi ang Cao, Congyue Deng, Rika Antonova, Shuran Song, and Jeannette Bohg. Equibot: Sim(3)-equivariant diffusion policy for generalizable and data efficient learning, 2024. 2
- [41] Tianwei Yin, Michaël Gharbi, Taesung Park, Richard Zhang, Eli Shechtman, Fredo Durand, and William T Freeman. Improved distribution matching distillation for fast image synthesis. 2024. 3
- [42] Tianwei Yin, Michaël Gharbi, Richard Zhang, Eli Shechtman, Frédo Durand, William T Freeman, and Taesung Park. One-step diffusion with distribution matching distillation. 2024. 5
- [43] Tianhe Yu, Deirdre Quillen, Zhanpeng He, Ryan Julian, Karol Hausman, Chelsea Finn, and Sergey Levine. Meta-world: A benchmark and evaluation for multi-task and meta reinforcement learning. 2019. 6, 1
- [44] Yanjie Ze, Zixuan Chen, Wenhao Wang, Tianyi Chen, Xialin He, Ying Yuan, Xue Bin Peng, and Jiajun Wu. Generalizable humanoid manipulation with improved 3d diffusion policies. *arXiv preprint arXiv:2410.10803*, 2024. 2, 3
- [45] Yanjie Ze, Gu Zhang, Kangning Zhang, Chenyuan Hu, Muhan Wang, and Huazhe Xu. 3d diffusion policy: Generalizable visuomotor policy learning via simple 3d representations. 2024. 2, 3, 6, 7, 8, 1
- [46] Qinglun Zhang, Zhen Liu, Haoqiang Fan, Guanghui Liu, Bing Zeng, and Shuaicheng Liu. Flowpolicy: Enabling fast and robust 3d flow-based policy via consistency flow matching for robot manipulation, 2024. 2
- [47] Tony Z. Zhao, Vikash Kumar, Sergey Levine, and Chelsea Finn. Learning fine-grained bimanual manipulation with low-cost hardware, 2023. 2
- [48] Wenliang Zhao, Lujia Bai, Yongming Rao, Jie Zhou, and Jiwen Lu. Unipc: A unified predictor-corrector framework for fast sampling of diffusion models, 2023. 3
- [49] Yuke Zhu, Josiah Wong, Ajay Mandlekar, Roberto Martín-Martín, Abhishek Joshi, Soroush Nasiriany, and Yifeng Zhu. robosuite: A modular simulation framework and benchmark for robot learning, 2022. 6

# Score and Distribution Matching Policy: Advanced Accelerated Visuomotor Policies via Matched Distillation

## Supplementary Material

### A. Implementation Details

**Task suite.** For the simulation experiments, to demonstrate the effectiveness of our method and ensure that our benchmarking is not influenced by the simulation environment, we conducted a comprehensive evaluation across 57 robotic tasks in three domains. These include 3 tasks from Adroit[21], 4 tasks from DexArt[1], and 50 tasks from MetaWorld[43], with the MetaWorld tasks categorized by varying difficulty levels. Table 6 provides a brief overview, highlighting the differences in action dimensions, object morphology, and robot models among these tasks.

Table 6. **Task suite.** Summarized 57 tasks in the simulation benchmark, including information on domains, robot models, object types, simulators, action dimensions, and the number of tasks. This demonstrates the diversity of the simulation benchmark in terms of robot types, object morphologies, simulators, and action dimensions, ensuring comprehensive evaluation across different scenarios.

Domain	Robot	Object	Simulator	Action Dimensions	Tasks Numbers
Adroit	Shadow	Rigid/Articulated	MuJoCo	28	3
DexArt	Allegro	Articulated	Sapien	22	4
MetaWorld	Gripper	Rigid/Articulated	MuJoCo	4	50

**Algorithm introduction.** Algorithm 1 provides a detailed explanation of the training process for the SDM Policy, with a particular focus on the updated details of gradient optimization and diffusion optimization.

### B. All Results of Simulation Experiments

To better demonstrate the effectiveness of SDM Policy, we provide a detailed presentation of the results related to task success rates, inference speed, and action performance discussed in the main text. The detailed results for individual tasks are separately reported in Table 7, Table 8, Table 9. It is important to note that we did not calculate inference speed and action quality for tasks with a success rate of 0, as such data would be meaningless. In the subsequent tables, we uniformly represent these cases as “Failure”.

For task execution performance, we provide a more detailed illustration in Figure 7 and Figure 8. For certain tasks, our SDM Policy better captures the action execution of the teacher model, while the consistency distillation method may encounter task execution failures. For the demonstration of these tasks, we adopt a unified intermediate state of epochs, which indirectly proves the effectiveness of our method in terms of learning efficiency mentioned in Section 5.2 in the main text.

---

### Algorithm 1 SDM Policy Training Procedure

---

**Input:** One-step generator  $G_\theta$ , Pretrained Target Network  $P_\theta$ , Dynamically-learned Network  $D_\theta$ , and pre-trained diffusion policies  $\pi_\theta$

**Output:** Trained generator  $G_\theta$ .

**Initialization:** Initialize generator  $G_\theta$ ,  $P_\theta$ , and  $D_\theta$  from pretrained diffusion policies  $\pi_\theta$  ( $G_\theta \leftarrow \pi_\theta$ ,  $P_\theta \leftarrow \pi_\theta$ ,  $D_\theta \leftarrow \pi_\theta$ ).

```
1: while not converged do
2:   // Generate action
3:   Sample  $z \sim \mathcal{N}(0, I)$ 
4:    $a_{G(\theta)}^0 \leftarrow G_\theta(z)$ 
5:   // Add noise to action
6:    $a_{G(\theta)}^t \leftarrow a_{G(\theta)}^0$ 
7:   // Compute the KL-divergence loss (Eq. 2)
8:   Compute the  $\mathcal{D}_{\text{KL}}$  between  $D_\theta$  and  $P_\theta$ 
9:   // Compute score function
10:   $s_{P_\theta}(a_{G(\theta)}^t) \leftarrow \log p_{P_\theta}(a_{G(\theta)}^t)$  (Eq. 3)
11:   $s_{D_\theta}(a_{G(\theta)}^t) \leftarrow \log p_{D_\theta}(a_{G(\theta)}^t)$  (Eq. 3)
12:  // Compute the one-step generator loss to update  $G_\theta$ 
    (Eq. 5)
13:  Compute the  $\mathcal{L}_{\text{one-step generator}}$  between  $D_\theta$  and  $P_\theta$ 
14:  // Compute the diffusion loss to update  $D_\theta$  (Eq. 6)
15:  Compute the  $\mathcal{L}_{\text{diffusion}}$  between  $D_\theta$  and  $G_\theta$ 
16:  if iter mod  $c == 0$  then
17:    Update  $G, D_\theta$ 
18:  else
19:    Update  $D_\theta$ 
20:  end if
21: end while
```

---

### C. SDM Policy in 2D Scene

To better demonstrate the effectiveness and generality of our method, we also performed distillation on the Diffusion Policy[4], achieving similarly leading results. This ensures the applicability of our approach to the distillation of various diffusion policies. While previous works have demonstrated the superiority of 3D Diffusion Policy [45], the use of 3D often entails significantly higher computational costs, making it unsuitable for various task scenarios and incapable of meeting the computational demands of lightweight embedded devices such as NVIDIA Jetson. Therefore, we believe that validating our method on Diffusion Policy [4] is crucial.

Table 7. **Detailed results for 57 simulated tasks with success rates.** We evaluated 57 challenging tasks using 3 random seeds and reported the average success rate (%) and standard deviation for each domain individually. \* indicates our reproduction of the task. Our SDM policy outperforms the current state-of-the-art models in one-step inference, achieving better results than Consistency Distillation and coming closer to the performance of the teacher model, demonstrating its effectiveness.

Alg \ Task	Adroit			DexArt				Meta-World (Easy)			
	Hammer	Door	Pen	Laptop	Faucet	Toilet	Bucket	Button Press	Coffee Button	Plate Slide	Back Side
Diffusion Policy	45 ± 5	37 ± 2	13 ± 2	69 ± 4	23 ± 8	58 ± 2	46 ± 1	99 ± 1	99 ± 1		100 ± 0
3D Diffusion Policy	100 ± 0	62 ± 4	43 ± 6	83 ± 1	63 ± 2	82 ± 4	46 ± 2	100 ± 0	100 ± 0		100 ± 0
3D Diffusion Policy*	100 ± 0	75 ± 3	48 ± 3	80 ± 2	34 ± 5	74 ± 4	29 ± 2	100 ± 0	100 ± 0		100 ± 0
ManiCM*	100 ± 0	68 ± 1	49 ± 4	83 ± 2	34 ± 0	74 ± 1	36 ± 4	100 ± 0	100 ± 0		100 ± 0
SDM Policy	100 ± 0	73 ± 2	49 ± 4	83 ± 2	38 ± 1	72 ± 2	31 ± 3	100 ± 0	100 ± 0		100 ± 0

Alg \ Task	Meta-World (Easy)					
	Button Press Topdown	Button Press Topdown Wall	Button Press Wall	Peg Unplug Side	Door Close	Door Lock
Diffusion Policy	98 ± 1	96 ± 3	97 ± 3	74 ± 3	100 ± 0	86 ± 8
3D Diffusion Policy	100 ± 0	99 ± 2	99 ± 1	75 ± 5	100 ± 0	98 ± 2
3D Diffusion Policy*	99 ± 1	96 ± 3	100 ± 0	93 ± 3	100 ± 0	96 ± 3
ManiCM*	100 ± 0	96 ± 2	98 ± 3	71 ± 15	100 ± 0	98 ± 2
SDM Policy	98 ± 2	99 ± 1	100 ± 0	74 ± 19	100 ± 0	96 ± 2

Alg \ Task	Meta-World (Easy)							
	Door Open	Door Unlock	Drawer Close	Drawer Open	Faucet Close	Faucet Open	Handle Press	Handle Pull
Diffusion Policy	98 ± 3	98 ± 3	100 ± 0	93 ± 3	100 ± 0	100 ± 0	81 ± 4	27 ± 22
3D Diffusion Policy	99 ± 1	100 ± 0	100 ± 0	100 ± 0	100 ± 0	100 ± 0	100 ± 0	53 ± 11
3D Diffusion Policy*	100 ± 0	100 ± 0	100 ± 0	100 ± 0	100 ± 0	100 ± 0	100 ± 0	52 ± 8
ManiCM*	100 ± 0	82 ± 16	100 ± 0	100 ± 0	100 ± 0	100 ± 0	100 ± 0	10 ± 10
SDM Policy	100 ± 0	100 ± 0	100 ± 0	100 ± 0	99 ± 1	100 ± 0	100 ± 0	28 ± 11

Alg \ Task	Meta-World (Easy)							
	Handle Press Side	Handle Pull Side	Lever Pull	Plate Slide	Plate Slide Back	Dial Turn	Reach	Reach Wall
Diffusion Policy	100 ± 0	23 ± 17	49 ± 5	83 ± 4	99 ± 0	63 ± 10	18 ± 2	59 ± 7
3D Diffusion Policy	100 ± 0	85 ± 3	79 ± 8	100 ± 1	99 ± 0	66 ± 1	24 ± 1	68 ± 3
3D Diffusion Policy*	0 ± 0	82 ± 5	84 ± 8	100 ± 0	100 ± 0	91 ± 0	26 ± 3	74 ± 3
ManiCM*	0 ± 0	48 ± 11	82 ± 7	100 ± 0	96 ± 5	84 ± 2	33 ± 3	62 ± 5
SDM Policy	0 ± 0	68 ± 6	84 ± 9	100 ± 0	100 ± 0	88 ± 3	34 ± 3	80 ± 1

Alg \ Task	Meta-World (Easy)			Meta-World (Medium)				
	Plate Slide Side	Window Close	Window Open	Basketball	Bin Picking	Box Close	Coffee Pull	Coffee Push
Diffusion Policy	100 ± 0	100 ± 0	100 ± 0	85 ± 6	15 ± 4	30 ± 5	34 ± 7	67 ± 4
3D Diffusion Policy	100 ± 0	100 ± 0	100 ± 0	98 ± 2	34 ± 30	42 ± 3	87 ± 3	94 ± 3
3D Diffusion Policy*	100 ± 0	100 ± 0	99 ± 1	100 ± 0	56 ± 14	59 ± 5	79 ± 2	96 ± 2
ManiCM*	100 ± 0	100 ± 0	80 ± 26	4 ± 4	49 ± 17	73 ± 2	68 ± 18	96 ± 3
SDM Policy	100 ± 0	100 ± 0	78 ± 18	28 ± 26	55 ± 13	61 ± 3	72 ± 9	97 ± 2

Alg \ Task	Meta-World (Medium)						Meta-World (Hard)		
	Hammer	Peg Insert Side	Push Wall	Soccer	Sweep	Sweep Into	Assembly	Hand Insert	Pick Out of Hole
Diffusion Policy	15 ± 6	34 ± 7	20 ± 3	14 ± 4	18 ± 8	10 ± 4	15 ± 1	0 ± 0	0 ± 0
3D Diffusion Policy	76 ± 4	69 ± 7	49 ± 8	18 ± 3	96 ± 3	15 ± 5	99 ± 1	14 ± 4	14 ± 9
3D Diffusion Policy*	100 ± 0	79 ± 4	78 ± 5	23 ± 4	92 ± 4	38 ± 9	100 ± 0	28 ± 8	44 ± 3
ManiCM*	98 ± 2	75 ± 8	31 ± 7	27 ± 3	54 ± 16	37 ± 13	87 ± 3	28 ± 15	30 ± 16
SDM Policy	98 ± 2	83 ± 5	83 ± 4	25 ± 2	90 ± 6	32 ± 15	100 ± 0	24 ± 14	34 ± 24

Alg \ Task	Meta-World (Hard)			Meta-World (Very Hard)					Average
	Pick Place	Push	Push Back	Shelf Place	Disassemble	Stick Pull	Stick Push	Pick Place Wall	
Diffusion Policy	0 ± 0	30 ± 3	0 ± 0	11 ± 3	43 ± 7	11 ± 2	63 ± 3	5 ± 1	55.5 ± 3.58
3D Diffusion Policy	12 ± 4	51 ± 3	0 ± 0	17 ± 10	69 ± 4	27 ± 8	97 ± 4	35 ± 8	72.6 ± 3.20
3D Diffusion Policy*	0 ± 0	56 ± 5	0 ± 0	47 ± 2	91 ± 4	67 ± 0	100 ± 0	74 ± 4	76.1 ± 2.32
ManiCM*	0 ± 0	55 ± 2	0 ± 0	48 ± 3	87 ± 3	63 ± 2	100 ± 0	37 ± 16	69.0 ± 4.60
SDM Policy	0 ± 0	57 ± 0	100 ± 0	51 ± 4	86 ± 10	68 ± 10	0 ± 0	53 ± 12	74.8 ± 4.51

Table 8. **Detailed results for 57 simulated tasks with inference speed.** We evaluated 57 challenging tasks using 3 random seeds and reported the average inference speed (Hz) for each domain individually. \* indicates our reproduction of that task, and to ensure fairness we must use the same computing resource configuration. Our SDM policy outperforms the current state-of-the-art models in one-step inference, achieving better results than Consistency Distillation, demonstrating its effectiveness.

Alg \ Task	Adroit			DexArt				Meta-World (Easy)			
	Hammer	Door	Pen	Laptop	Faucet	Toilet	Bucket	Button Press	Coffee Button	Plate Slide	Back Side
3D Diffusion Policy*	10.78Hz	11.40Hz	10.18Hz	10.19Hz	10.58Hz	10.72Hz	9.99Hz	10.20Hz	10.25Hz	10.31Hz	
ManiCM*	74.36Hz	48.80Hz	49.51Hz	72.50Hz	78.19Hz	70.95Hz	71.12Hz	50.69Hz	53.56Hz	66.35Hz	
SDM Policy	76.56Hz	48.80Hz	47.04Hz	70.23Hz	82.85Hz	75.20Hz	74.08Hz	49.96Hz	59.47Hz	83.08Hz	

Alg \ Task	Meta-World (Easy)						
	Button Press Topdown	Button Press Topdown Wall	Button Press Wall	Peg Unplug Side	Door Close	Door Lock	
3D Diffusion Policy*	10.28Hz	10.27Hz	10.40Hz	10.12Hz	10.35Hz	10.14Hz	
ManiCM*	52.49Hz	53.16Hz	53.00Hz	55.64Hz	51.78Hz	53.97Hz	
SDM Policy	52.51Hz	51.85Hz	52.56Hz	66.78Hz	51.42Hz	54.15Hz	

Alg \ Task	Meta-World (Easy)							
	Door Open	Door Unlock	Drawer Close	Drawer Open	Faucet Close	Faucet Open	Handle Press	Handle Pull
3D Diffusion Policy*	10.12Hz	10.16Hz	10.65Hz	10.19Hz	10.39Hz	10.28Hz	10.31Hz	10.20Hz
ManiCM*	50.93Hz	66.25Hz	51.97Hz	54.03Hz	53.73Hz	50.98Hz	51.82Hz	51.59Hz
SDM Policy	50.51Hz	52.09Hz	52.23Hz	50.89Hz	56.25Hz	51.92Hz	52.13Hz	89.75Hz

Alg \ Task	Meta-World (Easy)								
	Handle Press Side	Handle Pull Side	Lever Pull	Plate Slide	Plate Slide Back	Dial Turn	Reach	Reach Wall	
3D Diffusion Policy*	Failure	10.25Hz	10.10Hz	10.27Hz	10.12Hz	10.27Hz	10.04Hz	10.11Hz	
ManiCM*	Failure	51.73Hz	51.76Hz	50.78Hz	51.21Hz	83.92Hz	55.92Hz	51.80Hz	
SDM Policy	Failure	53.35Hz	55.16Hz	81.32Hz	83.71Hz	87.74Hz	88.08Hz	64.95Hz	

Alg \ Task	Meta-World (Easy)				Meta-World (Medium)				
	Plate Slide Side	Window Close	Window Open		Basketball	Bin Picking	Box Close	Coffee Pull	Coffee Push
3D Diffusion Policy*	10.33Hz	10.55Hz	10.50Hz		10.64Hz	11.42Hz	10.57Hz	11.54Hz	11.73Hz
ManiCM*	50.56Hz	63.4Hz	52.88Hz		56.07Hz	70.41Hz	64.61Hz	64.56Hz	51.86Hz
SDM Policy	81.42Hz	50.50Hz	55.60Hz		52.04Hz	79.31Hz	64.41Hz	64.80Hz	91.63Hz

Alg \ Task	Meta-World (Medium)						Meta-World (Hard)		
	Hammer	Peg Insert Side	Push Wall	Soccer	Sweep	Sweep Into	Assembly	Hand Insert	Pick Out of Hole
3D Diffusion Policy*	10.38Hz	10.31Hz	10.55Hz	10.57Hz	10.48Hz	10.46Hz	10.53Hz	10.80Hz	10.60Hz
ManiCM*	49.94Hz	68.25Hz	61.42Hz	54.44Hz	54.16Hz	65.1Hz	62.67Hz	69.48Hz	66.51Hz
SDM Policy	49.32Hz	57.06Hz	50.38Hz	47.82Hz	52.07Hz	51.78Hz	65.92Hz	53.36Hz	58.91Hz

Alg \ Task	Meta-World (Hard)				Meta-World (Very Hard)					Average
	Pick Place	Push	Push Back	Shelf Place	Disassemble	Stick Pull	Stick Push	Pick Place Wall		
3D Diffusion Policy*	Failure	10.75Hz	Failure	10.56Hz	10.46Hz	10.40Hz	10.54Hz	10.69Hz	10.39Hz	
ManiCM*	Failure	65.80Hz	Failure	72.32Hz	54.18Hz	54.92Hz	51.18Hz	53.18Hz	58.48Hz	
SDM Policy	Failure	85.47Hz	Failure	54.27Hz	51.06Hz	52.90Hz	49.57Hz	52.52Hz	61.75Hz	

## C.1. Experimental Setup

**Datasets.** We conducted experimental validation on the Robomimic [19] dataset, we selected the task 'Square', which is considered more challenging for evaluation, while excluding the simpler tasks, Lift and Can.

**Baselines.** To align with the experimental setup in the main text and demonstrate the effectiveness of our SDM Policy model in balancing fast inference speed and accurate action quality, we reproduced the original Diffusion Policy [4] and the Consistency Policy [20], which adopts consistency distillation methods, as baselines for comparison.

**Evaluation metrics.** During the evaluation, we observed some variations in the success rates across different environment initializations. For this experiment, we ran 3 random seeds, specifically seeds 42, 43, and 44, to mitigate the impact of performance fluctuations. We report the average peak success rate across the three random seeds for each method during training.

## C.2. Efficiency and Effectiveness

To showcase the effectiveness of our method, we thoroughly evaluated it based on four critical metrics: task suc-

Table 9. **Detailed results for 57 simulated tasks with action.** We used 3 random seeds to compare the learning effects of action generation on a 57 challenging task during training, and reported the mean action error and standard deviation in the three domains. \* indicates our reproduction of that task, and to ensure fairness we must use the same computing resource configuration. Our SDM policy outperforms the current state-of-the-art models in one-step inference, achieving better results than Consistency Distillation, demonstrating its effectiveness.

Alg \ Task	Adroit			DexArt				Meta-World (Easy)		
	Hammer	Door	Pen	Laptop	Faucet	Toilet	Bucket	Button Press	Coffee Button	Plate Slide Back Side
3D Diffusion Policy*	0.041 ± 0.025	0.054 ± 0.029	0.055 ± 0.038	0.020 ± 0.007	0.016 ± 0.005	0.019 ± 0.005	0.014 ± 0.004	0.077 ± 0.053	0.034 ± 0.007	0.025 ± 0.008
ManiCM*	0.033 ± 0.000	0.016 ± 6.803	0.490 ± 0.001	0.010 ± 7.370	0.009 ± 3.659	0.010 ± 9.961	0.010 ± 4.237	0.171 ± 0.009	0.066 ± 0.001	0.011 ± 0.000
SDM Policy	0.032 ± 9.204	0.006 ± 2.703	0.500 ± 0.000	0.002 ± 0.103	0.017 ± 0.001	0.007 ± 0.001	0.012 ± 0.000	0.141 ± 0.003	0.069 ± 0.001	0.007 ± 4.247

Alg \ Task	Meta-World (Easy)					
	Button Press Topdown	Button Press Topdown Wall	Button Press Wall	Peg Unplug Side	Door Close	Door Lock
3D Diffusion Policy*	0.102 ± 0.115	0.067 ± 0.076	0.110 ± 0.040	0.121 ± 0.063	0.109 ± 0.276	0.257 ± 0.243
ManiCM*	0.158 ± 0.002	0.166 ± 0.001	0.173 ± 0.002	0.195 ± 0.006	0.776 ± 0.021	0.186 ± 0.007
SDM Policy	0.114 ± 0.001	0.153 ± 0.001	0.140 ± 0.001	0.200 ± 0.004	0.056 ± 0.000	0.0143 ± 0.003

Alg \ Task	Meta-World (Easy)							
	Door Open	Door Unlock	Drawer Close	Drawer Open	Faucet Close	Faucet Open	Handle Press	Handle Pull
3D Diffusion Policy*	0.081 ± 0.070	0.193 ± 0.168	0.124 ± 0.138	0.057 ± 0.012	0.151 ± 0.126	0.149 ± 0.124	0.394 ± 0.539	0.612 ± 1.355
ManiCM*	0.092 ± 0.001	0.339 ± 0.011	0.676 ± 0.011	0.095 ± 0.002	0.295 ± 0.007	0.308 ± 0.006	0.884 ± 0.098	2.888 ± 0.142
SDM Policy	0.089 ± 0.001	0.296 ± 0.005	0.626 ± 0.017	0.100 ± 0.001	0.295 ± 0.002	0.248 ± 0.002	0.877 ± 0.052	2.622 ± 0.205

Alg \ Task	Meta-World (Easy)							
	Handle Press Side	Handle Pull Side	Lever Pull	Plate Slide	Plate Slide Back	Dial Turn	Reach	Reach Wall
3D Diffusion Policy*	Failure	1.355 ± 8.273	0.156 ± 0.069	0.096 ± 0.021	0.032 ± 0.009	0.050 ± 0.009	0.006 ± 0.001	0.080 ± 0.029
ManiCM*	Failure	2.414 ± 0.236	0.042 ± 0.001	0.213 ± 0.002	0.046 ± 0.001	0.055 ± 0.000	0.041 ± 4.470	0.045 ± 0.001
SDM Policy	Failure	2.298 ± 0.490	0.005 ± 8.085	0.163 ± 0.001	0.056 ± 0.000	0.040 ± 0.004	0.094 ± 0.014	0.019 ± 0.000

Alg \ Task	Meta-World (Easy)			Meta-World (Medium)				
	Plate Slide Side	Window Close	Window Open	Basketball	Bin Picking	Box Close	Coffee Pull	Coffee Push
3D Diffusion Policy*	0.137 ± 0.028	0.179 ± 0.208	0.351 ± 0.250	0.293 ± 0.276	0.183 ± 0.094	0.168 ± 0.092	0.045 ± 0.014	0.077 ± 0.017
ManiCM*	0.143 ± 0.007	0.230 ± 0.017	0.485 ± 0.030	0.539 ± 0.034	0.057 ± 0.002	0.037 ± 0.001	0.029 ± 0.000	0.050 ± 0.001
SDM Policy	0.157 ± 0.002	0.202 ± 0.003	0.521 ± 0.013	0.357 ± 0.004	0.027 ± 0.000	0.102 ± 0.022	0.017 ± 5.617	0.049 ± 0.001

Alg \ Task	Meta-World (Medium)				Meta-World (Hard)				
	Hammer	Peg Insert Side	Push Wall	Soccer	Sweep	Sweep Into	Assembly	Hand Insert	Pick Out of Hole
3D Diffusion Policy*	0.032 ± 0.010	0.327 ± 0.274	0.237 ± 0.224	0.035 ± 0.010	0.288 ± 0.236	0.261 ± 0.106	0.040 ± 0.011	0.087 ± 0.010	0.340 ± 0.174
ManiCM*	0.051 ± 0.001	0.101 ± 0.007	0.063 ± 0.001	0.024 ± 5.471	0.117 ± 0.010	0.059 ± 0.003	0.233 ± 0.018	0.044 ± 0.000	0.413 ± 0.008
SDM Policy	0.055 ± 0.000	0.089 ± 0.002	0.005 ± 2.332	0.004 ± 5.203	0.174 ± 0.007	0.038 ± 0.000	0.059 ± 0.000	0.036 ± 0.000	0.267 ± 0.003

Alg \ Task	Meta-World (Hard)			Meta-World (Very Hard)					Average
	Pick Place	Push	Push Back	Shelf Place	Disassemble	Stick Pull	Stick Push	Pick Place Wall	
3D Diffusion Policy*	Failure	0.040 ± 0.008	Failure	0.416 ± 0.377	0.107 ± 0.025	0.218 ± 0.120	0.088 ± 0.020	0.212 ± 0.217	0.166 ± 0.278
ManiCM*	Failure	0.056 ± 0.001	Failure	0.197 ± 0.011	0.089 ± 0.001	0.089 ± 0.002	0.123 ± 0.003	0.397 ± 0.039	0.270 ± 0.014
SDM Policy	Failure	0.044 ± 0.000	Failure	0.261 ± 0.005	0.076 ± 0.000	0.057 ± 0.000	0.102 ± 0.001	0.229 ± 0.012	0.234 ± 0.017

cess rate, learning efficiency, inference time, and action learning. The SDM Policy demonstrated exceptional performance across all these dimensions.

**High accuracy.** Table 10 presents the evaluation results for the Square task, comparing DDIM, EDM, Consistency Policy, and our SDM Policy. To ensure a fair comparison, DDIM and EDM were trained with the same number of epochs. Leveraging the conclusion about learning efficiency from section 5.2 in the main text, and to reduce dependence on computational resources, we trained our model using only 50 epochs. Our method achieved better experimental results compared to consistency distillation-based methods.

**Competitive inference speed.** Table 11 presents the evaluation inference time results for the Square task, comparing

Table 10. **Comparisons on success rate.** We evaluated the task using three random seeds and reported the average success rate (%) along with the standard deviation. Our SDM Policy outperformed the current state-of-the-art models in single-step inference, achieving better results than consistency distillation methods. This demonstrates the effectiveness of our approach in RGB-based vision-guided diffusion policies and highlights the generalizability of our SDM Policy model.

Policy	Epochs	NFE	square-ph
<b>DDIM</b>	400	10	88 ± 6
<b>EDM</b>	400	19	82 ± 9
<b>Consistency Policy</b>	50	1	64 ± 10
<b>SDM Policy</b>	50	1	66 ± 5

EDM, Consistency Policy, and our SDM Policy. The results

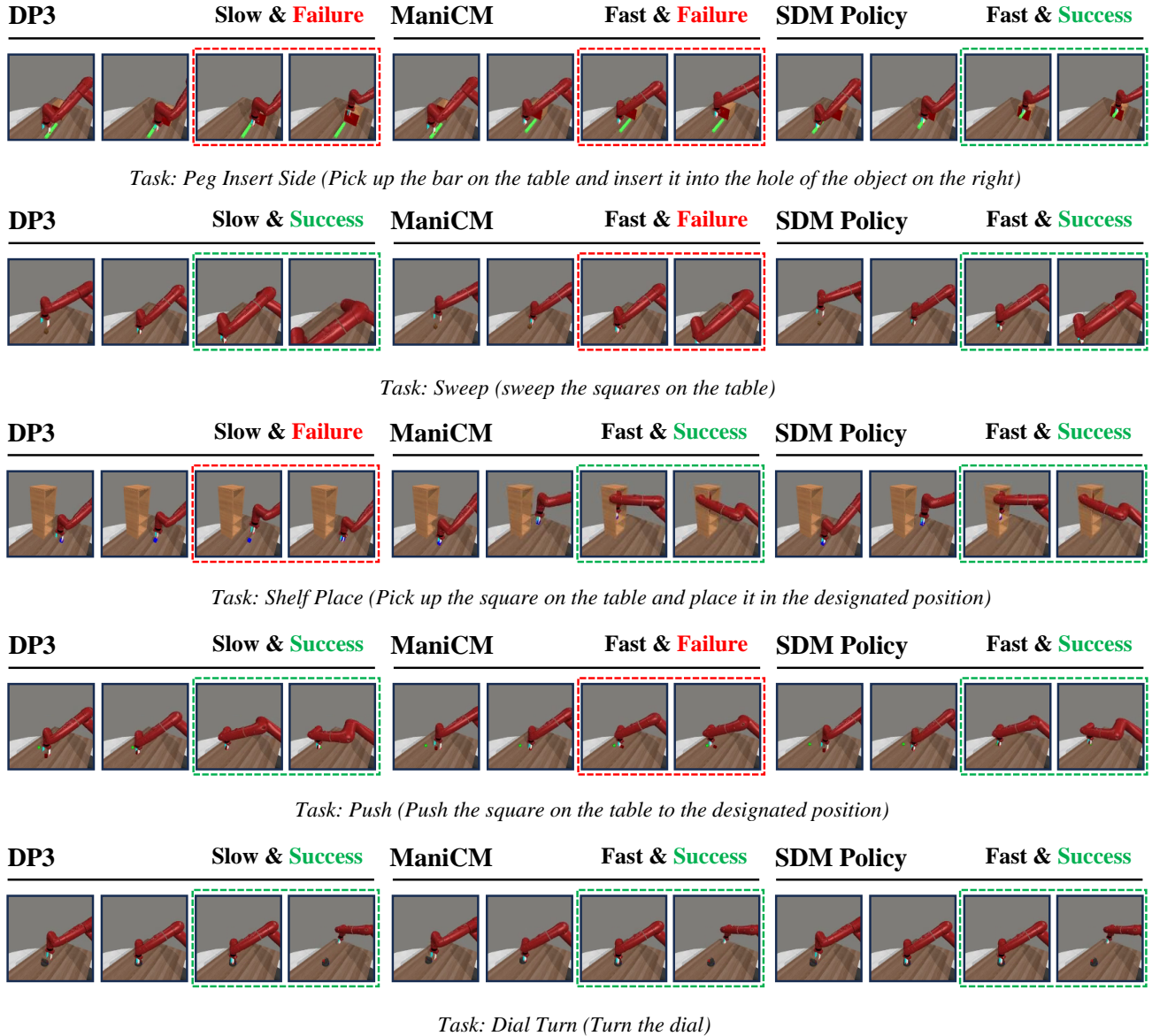


Figure 7. **Part 1 of the task execution visualization.** We conducted a detailed visualization of the performance on a subset of 57 tasks. Specifically, 10 tasks were randomly selected for demonstration and comparison based on the domain and task difficulty, proportionally representing the 57 tasks. This is the first part of the task performance visualization, focusing on tasks categorized as medium, hard, and very hard in MetaWorld. The demonstrations are taken from an intermediate state across all epochs, with red indicating task failure and green indicating task success. The dashed boxes highlight keyframes of either failures or successes. For most tasks, our SDM Policy can complete the tasks quickly and accurately, demonstrating the effectiveness of our method.

demonstrate that our method achieves a comparable performance to the current SOTA consistency distillation method while achieving over 18 times inference acceleration compared to the original EDM-based results.

**Precise and accurate action.** As shown in Table 12, we also found that the action quality learned by the SDM Policy is precise, and consistent with the current SOTA methods. This is in line with the previously mentioned higher

success rate and learning efficiency, further validating the effectiveness of our approach.

#### D. Further Discussion

This work has demonstrated that enforcing the minimization of the matching loss between two diffusion distributions provides a direct signal for training the generator, significantly improving distillation performance. The 57 ex-

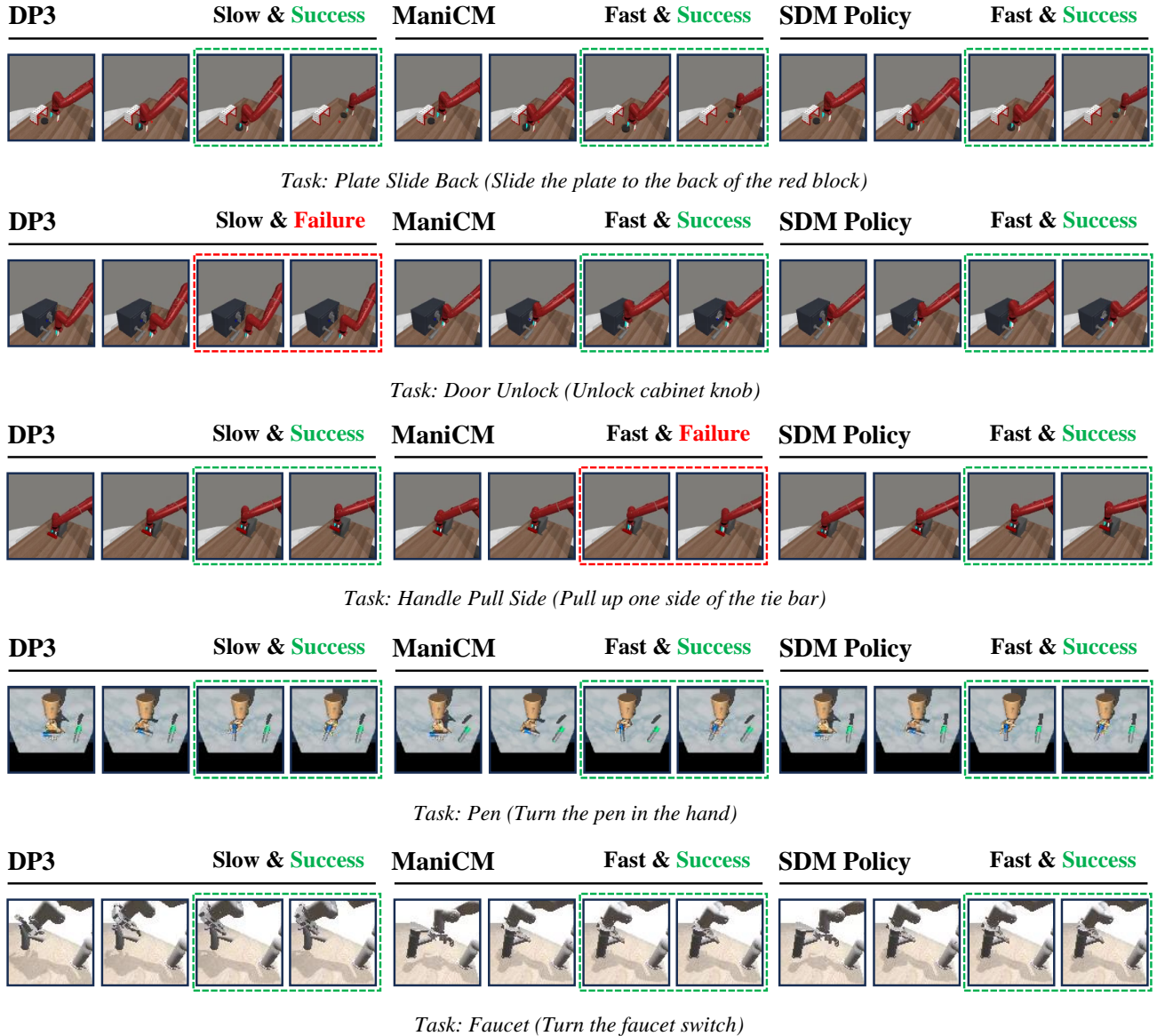


Figure 8. **Part 2 of the task execution visualization.** We conducted a detailed visualization of the performance on a subset of 57 tasks. Specifically, 10 tasks were randomly selected for demonstration and comparison based on the domain and task difficulty, proportionally representing the 57 tasks. This is the second part of the task performance visualization, focusing on tasks categorized as easy in MetaWorld, Adroit and DexArt. The demonstrations are taken from an intermediate state across all epochs, with red indicating task failure and green indicating task success. The dashed boxes highlight keyframes of either failures or successes. For most tasks, our SDM Policy can complete the tasks quickly and accurately, demonstrating the effectiveness of our method.

periments listed in the paper have shown that our method achieves a balance between fast inference speed and high-quality actions. Although we briefly discussed follow-up questions in the main text, we provide a more detailed description here.

First, our average task success rate does not exceed that of the teacher model DP3, with only a subset of tasks surpassing it. Overall, our method achieves performance closer

to the teacher model compared to consistency distillation methods. From an information-theoretic perspective, the distilled model trained through knowledge distillation incorporates more effective Knowledge Points and can simultaneously learn multiple Knowledge Points. This results in more stable optimization compared to models trained from scratch, where the teacher model learns sequentially. In future work, we will continue to explore this direction.



Table 11. **Comparisons on inference speed.** We evaluated the task using three random seeds and reported the average speed (Hz). Our SDM Policy outperformed the current state-of-the-art models in single-step inference, achieving better results than consistency distillation methods. This demonstrates the effectiveness of our approach in RGB-based vision-guided diffusion policies and highlights the generalizability of our SDM Policy model.

Policy	Epochs	NFE	square-ph
<b>EDM</b>	400	19	2.75Hz
<b>Consistency Policy</b>	50	1	51.77Hz
<b>SDM Policy</b>	50	1	49.13Hz

Table 12. **Comparisons on action.** We evaluated the task using three random seeds and reported the average action error and standard deviation. Our SDM Policy outperformed the current state-of-the-art models in single-step inference, achieving better results than consistency distillation methods. This demonstrates the effectiveness of our approach in RGB-based vision-guided diffusion policies and highlights the generalizability of our SDM Policy model.

Policy	Epochs	NFE	square-ph
<b>DDIM</b>	400	10	0.096 ± 0.029
<b>EDM</b>	400	19	0.092 ± 0.009
<b>Consistency Policy</b>	50	1	0.050 ± 0.001
<b>SDM Policy</b>	50	1	0.050 ± 0.000

In addition, based on the data obtained from testing 57 simulation tasks, our SDM Policy achieves an average speed of 61.75Hz, representing a 6x improvement compared to DP3’s 10.9Hz. For practical applications, extending our method to dynamic operations and tasks requiring high-frequency control is critical to adapting to more complex and unpredictable environments. For instance, dexterous hands operating on complex objects such as twisting bottle caps or grasping flexible objects require real-time feedback on the force and position of each finger to adjust the grasping policy dynamically. Precision operations such as threading a needle or assembling electronic components demand higher control accuracy, requiring real-time closed-loop perception and control during the inference process. For grippers, tasks involving dynamic scenarios such as grabbing moving targets on a fast conveyor belt necessitate higher inference frequency to maintain success rates. Additionally, during the grasping process, objects may suddenly slip or change position, and fast inference is essential to quickly adjust actions when environmental feedback changes. These discussions underscore the significance of our method’s exploration of fast inference and high-quality action learning. In future work, we will further investigate and address these scenarios and discussions.